Extra-large Gα protein (XLαs) deficiency causes severe adenine-induced renal injury with massive FGF23 elevation

Julia Matthias[1], Qiuxia Cui[1], Lauren T. Shumate[1], Antonius Plagge[2], Qing He[1],[#],

and Murat Bastepe[1]*

[1]Endocrine Unit, Department of Medicine, Massachusetts General Hospital and Harvard

Medical School, Boston, MA, USA

[2]Department of Cellular and Molecular Physiology, Institute of Translational Medicine,

University of Liverpool, Liverpool, United Kingdom

[#]**Address correspondence to:**

1) Murat Bastepe, MD, PhD
50 Blossom St. Thier 10
Boston, MA 02114, U.S.A
Email: bastepe@helix.mgh.harvard.edu

2) Qing He, PhD
50 Blossom St. Thier 10
Boston, MA 02114, U.S.A
Email: qing.he@mgh.harvard.edu

Abstract

Fibroblast growth factor-23 (FGF23) is critical for phosphate and vitamin D homeostasis. Cellular and molecular mechanisms underlying FGF23 production remain poorly defined. The extra-large Gα subunit (XLαs) is a variant of the stimulatory G protein alpha-subunit (Gsα), which mediates the stimulatory action of parathyroid hormone in skeletal FGF23 production. XLαs ablation causes diminished FGF23 levels in early postnatal mice. Herein we found that plasma FGF23 levels were comparable in adult XLαs knockout (XLKO) and WT littermates. Upon adenine-rich diet-induced renal injury, a model of chronic kidney disease, both mice showed increased levels of plasma FGF23. Unexpectedly, XLKO mice had markedly higher FGF23 levels than WT mice, with higher BUN and more severe tubulopathy. FGF23 mRNA levels increased substantially in bone and bone marrow in both genotypes; however, the levels in bone were markedly higher than in bone marrow. In XLKO mice, a positive linear correlation was observed between plasma FGF23 and bone, but not bone marrow, FGF23 mRNA levels, suggesting that bone, rather than bone marrow, is an important contributor to severely elevated FGF23 levels in this model. Upon folic acid injection, a model of acute kidney injury, XLKO and WT mice exhibited similar degrees of tubulopathy; however, plasma phosphate and FGF23 elevations were modestly blunted in XLKO males, but not in females, compared to WT counterparts. Our findings suggest that XLαs ablation does not substantially alter FGF23 production in adult mice but increases susceptibility to adenine-induced kidney injury, causing severe FGF23 elevations in plasma and bone.

Keywords

2

Introduction

An important hormone regulating phosphate and vitamin D homeostasis is fibroblast growth factor 23 (FGF23) (1,2). Pro-FGF23 is synthesized as a 251 amino acid protein in the bone tissue by osteoblasts and osteocytes and is cleaved intracellularly to form the mature FGF23 protein, which is either secreted intact (iFGF23) or inactivated by another intracellular cleavage step, to form the inactive N- and C-terminal fragments (3). iFGF23 then inhibits the reabsorption of phosphate from the glomerular filtrate and diminishes the synthesis of the bioactive vitamin D metabolite 1,25-dihydroxyvitamin D3 in the renal tubule (4). Dysregulated actions of FGF23 is associated with several human genetic and acquired disorders. For example, patients with X-linked hypophosphatemic rickets produce excess levels of FGF23 in bone and thus display renal phosphate wasting (5). Conversely, patients with familial hyperphosphatemic tumoral calcinosis display inactivating mutations in GALNT3 or FGF23 and are therefore deficient for iFGF23 levels (6). In addition, FGF23 levels in the circulation rise dramatically as a result of renal failure (7). Although this elevation is beneficial in early stages of the kidney injury by preventing soft tissue mineralization, the highly increased FGF23 levels in end-stage renal disease have been found to correlate with the occurrence of left ventricular hypertrophy and the increased risk of cardiovascular events (8,9), thus contributing to the morbidity and mortality in patients with chronic kidney disease (CKD). The mechanisms underlying FGF23 production remain incompletely defined.

Osteocytes and osteoblasts in bone are already known to be important producers of FGF23, providing a substantial portion of serum FGF23 at baseline and in response to a high phosphate challenge (10). Several other tissues have also been shown to contribute to FGF23 production

3

under different conditions, such as in inflammation and in response to kidney injury (1,11-14). Mouse studies have shown that bone marrow, which contains hematopoietic and mesenchymal stem cells, is capable of producing FGF23 upon blood loss-induced erythropoietin (EPO) expression or in response to EPO injection, with a more significant or comparable contribution compared to bone, respectively (14-16). On the other hand, a recent study demonstrated that multiple tissues, including bone, contribute to the elevation of FGF23 in a folic acid-induced acute kidney injury (AKI) model but observed no elevation of FGF23 mRNA in bone marrow (17), suggesting that bone marrow is unlikely to be a source of FGF23 in renal failure. Relative contributions of bone and bone marrow to the excess FGF23 levels in the setting of CKD have remained uncertain.

Production of FGF23 is stimulated by a number of exogenous molecules, including 1,25-dihydroxyvitamin D, calcium, and leptin (18-20). Recently, inflammatory mediators, which are systemically increased in CKD, have also come to the focus of attention as stimulators of FGF23 synthesis (11,21,22). Another stimulator of osseous FGF23 production is parathyroid hormone (PTH), which acts via the stimulatory G protein Gsα, a ubiquitous signaling protein that mediates the actions of many hormones, autocrine and paracrine factors, and neurotransmitters via generation of cAMP (23-25). The PTH receptor can also couple to other heterotrimeric G protein alpha-subunits, including the extra-large variant of Gsα (XLαs) (26-28). XLαs can mimic Gsα with respect to cAMP generation and is expressed in bone marrow stromal cells, calvarial preosteoblasts, and osteocytes (28-31). It has been shown that early postnatal mice in which XLαs is ablated show hyperphosphatemia with diminished FGF23 levels in bone and in the circulation (32-34), indicating that XLαs is required for FGF23 production. However, unlike the action of Gsα in this regard, the action of XLαs in adulthood has remained unknown.

4

In this study, we investigated the role of XLαs in adult mice with respect to FGF23 production by examining XLαs knockout mice (XLKO) and wildtype littermates. Furthermore, to determine whether XLαs-mediated mechanisms are involved in kidney injury-induced FGF23 production, we employed a model of CKD involving the use of adenine-rich diet, as described (35). This model entails tubulointerstitial nephropathy due to the precipitation of highly insoluble adenine derivative 2,8-dihydroxyadenine in the renal parenchyma (36). While adult XLKO and wildtype (WT) littermates did not show significant differences in baseline plasma FGF23 levels, our findings have indicated that XLαs deficiency increases susceptibility to adenine-induced kidney injury. Moreover, we compared the levels of FGF23 mRNA in bone and bone marrow, revealing that bone, rather than bone marrow, is a substantial source of plasma FGF23 in the adenine-induced kidney injury model. We also employed the folic acid-induced AKI model, in which folic acid causes nephrotoxicity that leads to acute tubular necrosis (37). Folic acid injection resulted in a comparable degree of renal failure in XLKO and WT mice within 24 hours. In both CKD and AKI models, we have not detected differences between the two genotypes in the relationship between plasma FGF23 and phosphate levels.

Methods

Mice and Experimental Design

All animal experiments were conducted in accordance with the accepted standards of the Institutional Animal Care and Use Committee, and the studies were approved by The Massachusetts General Hospital Subcommittee on Research Animal Care.

Downloaded from https://academic.oup.com/endo/advance-article-abstract/doi/10.1210/endocr/bqz025/5638044 by University of Liverpool user on 27 November 2019

XLKO mice were generated by disrupting the first exon of XLαs on the paternal allele, as previously described (38), and maintained in the CD1 background. WT and XLKO mice had free access to water and a standard chow diet (0.9% phosphate, 0.6% calcium). At eight weeks of age, mice of each genotype were divided into two groups, of which one group was changed to receive an adenine-rich chow diet (0.2% adenine, 0.9% phosphate, 0.6% calcium) for a total period of 6 weeks. The mice and the food were weighed, and venous plasma samples were obtained from the tail vain on a weekly basis. Most male mice under the adenine group lost more than 25% of their weights before the completion of the study, and therefore, the analyses were performed only on female WT and XLKO mice. An aggravated disease progression of adenine-induced kidney disease in male compared to female rats has been observed previously (39). This finding is in accordance with observations in humans, as men show a faster progression towards end-stage renal disease compared to women before menopause (40), and might be caused by higher estrogen and ER-α activation in females (39). The mice were weighed weekly and supplemented subcutaneously with lactated ringer solution after 5% body weight loss compared to baseline weight at 0 weeks adenine/control-diet to reduce excessive water loss due to polyuria. The injected volume was equivalent to 4% of the current mouse weight and was given in two portions with four hours in between. AKI was induced in 12-week-old male and female XLKO and WT littermates by injecting 240mg/kg folic acid in sodium bicarbonate subcutaneously, as described (41). Vehicle injection was used as control. Blood samples were taken at baseline and at 2, 8 and 24 hours after injection. Mice were euthanized after 24 hours, and kidneys were morphologically examined for signs of kidney injury.

6

Histopathology

Kidneys were fixed in 10% paraformaldehyde, embedded in paraffin, and serially sectioned at 5 μm. Hematoxylin and eosin staining was performed using standard protocols. The tissue sectioning and staining were conducted at the Endocrine Unit, Massachusetts General Hospital Center for Skeletal Research.

Measurement of plasma biochemistries

Venous plasma samples were collected from tail vain puncture at different timepoints. Plasma phosphorous and BUN levels were determined with colorimetric assays, according to the manufacturer's protocols (Phosphate: Abcam Phosphate Assay Kit (Colorimetric); BUN: Stanbio™ BUN Liquid Reagent for Diagnostic Set). Plasma FGF23 levels were quantitated by using the Mouse/Rat FGF-23 (C-Term) ELISA Kit or the Mouse/Rat FGF-23 (Intact) ELISA Kit (both from Immutopics/Quidel).

cDNA synthesis and gene expression analysis

Cortical bone and bone marrow were separated by removing the epiphysis and metaphysis of the femur bone and flushing the diaphysis with PBS. Bone marrow and cortical bone samples were homogenized in Trizol. The total RNA was separated using the ThermoFisher TRIzol™ Reagent Kit and precipitated using the Qiagen RNeasy® Plus Mini Kit. Two μg RNA from each sample was run on a 1.5% Agarose gel to confirm RNA quality. cDNA was synthesized using the New England Biolabs ProtoScript II First strand cDNA synthesis kit according to the manufacturer's protocol. qRT-PCR analysis on FGF23 was performed using the Applied biosystems TaqMan Fast Advanced Master Mix and predesigned TaqMan gene expression assays Fgf23-FAM, Actb-

7

VIC (β-actin as reference control) and Gapdh-VIC (glyceraldehyde-3-phosphate dehydrogenase as reference control). qRT-PCR analysis on all other genes was performed with specific primers and the PowerUp SYBR Green Master Mix (Applied biosystems) with β-Actin as a reference gene. β-Actin (F: 5'-GATCTGGCACCACACCTTCT-3'; R: 5'-GGGGTGTTGAAGGTCTCAAA-3'), IL-6 (F: 5'-TACCACTTCACAAGTCGGAGGC-3'; R: 5'-CTGCAAGTGCATCATCGTTGTTC-3'), IL-1β (F: 5'-GGAGAACCAAGCAACGACAAAATA-3'; R: 5'-TGGGGAACTCTGCAGACTCAAAC-3'), Egr-1 (F: 5'-AGCGAACAACCCTATGAGCACC-3'; R: 5'-ATGGGAGGCAACCGAGTCGTTT-3'). Ratio of bone to bone marrow FGF23 mRNA levels (relative to β-Actin) were calculated for each study mouse by dividing the bone value to bone marrow value at baseline or at 6 weeks of adenine-rich diet.

Statistical analysis

Leven's F test was first performed to assess equality of variances between groups. If variances were equal, paired or unpaired Student's t test (two-tailed) was used for determining the statistical significance of the difference between two means. Otherwise, Welch's t test (two-tailed) was used. For multiple comparisons, Bonferroni correction was performed, i.e the P value was multiplied by the number of comparisons. Outliers in each data group were identified by using the Grubbs's test and excluded. Differences in plasma FGF23 values between different time points and between adenine-fed or folic acid-injected WT and XLKO mice were analyzed by using two-way repeated measures ANOVA. Pearson correlation coefficient was calculated to determine the degree with which two variables are linearly related. A P value smaller than 0.05

8

was considered statistically significant and represented as follows: *P < 0.05, **P < 0.01, ***P < 0.001, ****P<0.0001. Analyses were performed by using Prism 6 (GraphPad).

Results

XLKO mice develop a more advanced kidney injury upon adenine-rich diet

To understand the role of XLαs in kidney injury-induced FGF23 production we studied the XLαs knockout mice (XLKO). XLαs expression is monoallelic and occurs paternally in nearly all tissues, and XLKO mice carries the targeted gene only on the transcriptionally active paternal allele (38). After confirming the strong reduction of XLαs mRNA levels in bone (Fig 1A) and bone marrow (Fig 1B) of eight-week old XLKO mice, we measured the levels of total FGF23 and iFGF23 in the plasma. At baseline, total FGF23 levels (measured by the C-terminal FGF23 assay) in XLKO mice tended to be lower than the levels in WT littermates (Fig. 1C). While this result was in line with findings from early postnatal XLKO and WT pups (32), no difference was detectable in plasma iFGF23 levels between the two genotypes (Fig. 1D). In order to investigate whether XLαs is required for the FGF23 synthesis in CKD, we fed eight-week old XLKO and WT littermates a diet containing 0.2% adenine, as described previously (35,42). Many of the male XLKO mice had to be euthanized due to excessive weight loss two weeks after the start of the adenine diet (Fig 1E), and therefore, we had to limit our data collection to female XLKO and WT littermates. Among female mice, only one WT and one XLKO had to be excluded from the study due to excessive weight loss (Fig. 1F). As soon as one week after introducing the adenine-rich diet, pale spots could be found grossly on the kidney surface (Fig. 2A). After 6 weeks of adenine-rich diet, the whole kidneys appeared pale and showed morphological signs of atrophy with an irregular surface and a reduced size (Fig. 2B). The H&E staining of renal sections revealed extensive proximal and distal tubular luminal expansion, with more severe appearance

9

of tubulopathy in XLKO than in WT kidneys (Fig. 2C). A significant increase in plasma

phosphate levels was observed in both XLKO and WT littermates after six weeks of the adenine

diet (Fig. 2D). In addition, blood urea nitrogen (BUN) levels were elevated compared to

baseline in both genotypes, and the elevation was significantly more pronounced in XLKO than

in WT littermates (Fig. 2E). These findings confirmed the anticipated effect of adenine-rich diet

on the kidney and suggested that XLKO mice had more advanced kidney injury compared to WT

littermates. We found a slightly decreased adenine-rich food intake in XLKO mice compared to

WT littermates (WT control diet: 0.73±0.1g; WT adenine diet: 0.78±0.05g; XLKO control diet:

0.62±0.17g; XLKO adenine diet: 0.42±0.13g; values reflect the consumed amount of food per

day per gram mouse weight), thus making it unlikely that the more advanced kidney injury in

XLKO mice reflected increased consumption of the adenine-rich diet.

More advanced renal injury in XLKO mice is associated with higher plasma FGF23

levels

To characterize the FGF23 synthesis, we measured plasma total FGF23 levels, finding out

that an elevation was detectable as soon as one week after introducing the adenine-rich diet in

both XLKO (2,251 ± 766.7 pg/ml) and WT (994.2 ± 232.4 pg/ml) mice (Fig. 3A). At 6 weeks,

total FGF23 levels were markedly elevated, with higher levels in XLKO than WT

(104,206±21,741 vs. 18,430±3,379 pg/ml, p<0.0001; Fig. 3A). A mild increase of total FGF23

levels were also observed in control diet-fed animals (Fig. 3B). Plasma iFGF23 also measured

higher in both WT and XLKO mice fed the adenine-rich diet compared to control diet for six

weeks, with significantly higher levels in XLKO than WT mice (Fig. 3C). We then examined

the relationship between plasma total FGF23 and phosphate levels. At baseline, no linear

10

correlation was observed in either genotype (Fig. 3D). At 6 weeks, WT mice continued to show

no linear correlation between plasma total FGF23 and phosphate, whereas XLKO mice displayed

a statistically significant positive linear correlation (Fig. 3E). When all data – baseline and 6

weeks of adenine diet – are analyzed together, total FGF23 appeared to be linearly correlated

with plasma phosphate only in XLKO mice (Fig. 3F). Due to the wide variation of FGF23

values between baseline and 6 weeks of adenine diet, we then reperformed the linear regression

and correlation analysis after semi-log transformation of the data, i.e. logarithm of FGF23 vs.

phosphate. This analysis indicated a positive correlation in both WT and XLKO mice, and

furthermore, the linear relationship between log(FGF23) and phosphate in WT mice appeared to

be comparable to that in XLKO mice according to the statistical analysis of the difference

between the slopes (Fig. 3G).

Bone is an important contributor to plasma FGF23 levels in CKD

Both osteoblasts/osteocytes and bone marrow have been described as significant producers of

FGF23 (1,14,43,44). In order to characterize the synthesis of FGF23 in more detail, we extracted

femur bone and bone marrow samples from XLKO and WT mice after 6 weeks of adenine-rich

or control diet. Consistent with the plasma FGF23 levels, qRT-PCR analysis revealed increased

FGF23 mRNA levels in femur bone (Fig. 4A) and bone marrow samples (Fig. 4B) of mice fed

the adenine-rich diet. The values obtained from the femurs of adenine-fed XLKO mice showed

wide variation, and therefore, the difference between these mice and the control diet-fed XLKO

mice did not reach statistical significance (Fig 4A). In contrast, the increases observed in bone

marrow were significant in both WT and XLKO littermates (Fig, 4B). These findings were

confirmed by using another house-keeping gene as reference, i.e. Gapdh (Fig. 4C, D). Notably,

11

these experiments strongly suggested that the levels of FGF23 mRNA are markedly higher in bone than in bone marrow. Calculating the bone-to-bone marrow ratio in individual mice of either genotype, we found that, at baseline, the mean FGF23 mRNA level relative to β-actin was 28.6 ± 8.3 (95% confidence interval: 7.3-49.8) times higher in bone than in bone marrow. Six weeks after the adenine-rich diet, the FGF23 mRNA level continued to be dramatically higher in bone (Fig. 4E), with the mean bone-to-bone marrow ratio being 20.5 ± 7.7 (95% confidence interval: 1.5-39.4). When FGF23 mRNA was quantified relative to Gapdh, the level in bone following the six-week adenine-rich diet was 31.4 ± 10.5-fold (95% confidence interval: 5.8-56.9) higher than in bone marrow (Fig. 4E). To further investigate the contributions of bone and bone marrow to the plasma FGF23 levels, we analyzed the relationship between plasma FGF23 and tissue FGF23 mRNA levels. A positive correlation was observed in WT animals between plasma FGF23 and both bone (Fig. 5A) and bone marrow FGF23 mRNA levels (Fig. 5D). In contrast, a statistically significant correlation existed in XLKO animals only between plasma FGF23 and bone FGF23 mRNA levels (Fig. 5B, E). When the analysis was performed after pooling the values from both genotypes, plasma FGF23 correlated significantly with FGF23 mRNA in bone, but not in bone marrow (Fig. 5C, F). However, analyzing the logarithm of plasma FGF23 levels against bone marrow FGF23 mRNA levels, we detected a positive correlation in XLKO mice, as well as in pooled data from both of the genotypes (Fig. 5G, H).

Local inflammation is unlikely to drive the excess FGF23 production in bone and bone marrow in CKD

Inflammatory mediators have been shown to stimulate FGF23 expression (21,45,46). As CKD patients exhibit systemic inflammation, we subsequently addressed whether the observed

increase of FGF23 in bone and bone marrow samples reflect increased inflammation in these tissues. Analysis of inflammation markers isolated after 6 weeks of adenine-rich diet revealed a tendency of IL-1β mRNA levels to rise in XLKO (bone: 1.7 ± 0.29-fold; p=0.10; bone marrow: 1.84 ± 0.3-fold; p=0.06) but not in WT mice compared to control diet (Fig. 6A, B). The mRNA levels of IL6, which has been reported as an essential mediator of adenine-rich diet-induced FGF23 elevation (21), were modestly diminished in both bone and bone marrow of adenine-fed WT mice compared to control diet-fed WT mice (Fig. 6A, B). However, no significant differences were detected in IL6 mRNA levels in XLKO bone and bone marrow samples between control and adenine-rich diet (Fig. 6A, B). In contrast, both IL1β and IL6 and mRNA levels were markedly elevated in whole kidneys from WT and XLKO mice (Fig. 6C), verifying that the adenine-induced kidney injury was associated with increased renal inflammation.

Renal induction of FGF23 expression as a result of adenine-rich diet

It has recently been shown that FGF23 expression is induced in kidney tissue upon kidney injury (12,13). We thus sought to determine the FGF23 expression in WT and XLKO kidneys. While no FGF23 mRNA could be detected in whole kidneys of mice receiving the control diet, FGF23 mRNA was readily detectable in this tissue one week after introducing the adenine-diet in both genotypes and throughout the six-week experimental period (Fig. 7A, B). The actions of FGF23 in the kidneys are mediated by the activation of different pathways. One of these pathways initiates the suppression of renal Na/Pi cotransporters by increasing the renal expression of Egr1 through activation of the ERK1/2 signaling pathway (47). qRT-PCR experiments revealed an enhancement of renal Egr1 expression as soon as one week after introducing the adenine-rich diet in both WT and XLKO mice (Fig. 7C, D). Egr1 mRNA levels

13

in kidney correlated positively with plasma FGF23 levels (Fig. 7E), whereas no correlation was detected between renal Egr1 and FGF23 mRNA levels (Fig. 7F).

Folic acid induces comparable degrees of AKI in XLKO and WT mice with no apparent induction of renal FGF23 expression

To understand whether the increased susceptibility of XLKO mice to renal injury is specific to adenine-rich diet, we examined the effects of folic acid, an agent that leads to acute kidney injury. Within 24 hours after folic acid injection, plasma FGF23 levels rise markedly (41), and FGF23 mRNA levels increase in multiple tissues, including bone but not bone marrow (17). As expected, we observed a gradual increase of BUN in folic acid-injected female and male mice, and the levels were comparable at each time point between WT and XLKO (Fig. 8B, E), suggesting a similar degree of renal injury in both genotypes. Plasma phosphate also increased similarly in WT and XLKO mice, with modestly lower levels in XLKO males compared to WT males 24 hours after the injection (Fig. 8A, D). Plasma total FGF23 also rose gradually without significant differences between genotypes; however, male XLKO mice showed significantly lower FGF23 levels than WT males at 24 hours (Fig. 8C, F). Linear regression analysis of total FGF23 and phosphate levels did not reveal any significant differences between WT and XLKO mice, showing positive linear correlations (Fig. 9A, C). However, on semi-log transformation of data, the slope of the regression line was steeper in XLKO males, but not in females, than their WT counterparts (Fig. 9B, D), suggesting that phosphate might have a greater magnitude of effect on total FGF23 levels in XLKO males in the setting of acute kidney injury.

We also analyzed the kidneys of folic acid-injected mice with respect to the expression levels of FGF23 and inflammation markers. Unlike our findings in adenine-fed mice, we could not

14

detect renal FGF23 expression in control or folic acid-injected mice, regardless of the genotype.

IL6 mRNA levels in kidneys of folic acid-injected mice, on the other hand, were elevated (Fig.

10A, B); however, the elevation in WT females was not statistically significant (Fig. 10A).

Renal IL1β mRNA levels rose mildly in WT and XLKO females in response to folic acid-

injection, but the differences were not statistically significant (Fig. 10C). WT males, but not

XLKO males, displayed a slight, statistically significant elevation of renal IL1β mRNA (Fig.

10D). Renal Egr1 mRNA levels were elevated in folic acid-injected WT and XLKO mice

compared to controls (Fig. 10E, F); however, the difference in XLKO males did not reach

statistical significance.

Discussion

Based on our recent observations of reduced FGF23 plasma levels in early postnatal XLKO

mice, and based on the finding that XLαs is expressed in adult bone, we investigated the role of

this protein in renal injury-induced FGF23 production. We used an established model of CKD

involving an 0.2% adenine-containing diet. We chose to begin the diet in 8 week-old mice,

because the initial study that established this protocol in mice, as well as many pursuant studies,

had employed mice at this age and been able to reliably detect increases in FGF23 levels (35).

Although mice at this age have typically not reached skeletal maturity, this is unlikely to

confound our results, given that the control diet-fed WT and XLKO mice showed only a minor

increase in their FGF23 levels over the 6-week treatment period. In addition, we also measured

the difference in plasma phosphate levels in control diet-fed mice between 8 weeks and 14 weeks

(i.e. the end-point of our study), and revealed that, in keeping with findings in pediatric age

humans (48), both WT and XLKO mice showed a modest decline in plasma phosphate levels (-

15

0.572±0.14mM and -0.323±0.1mM in 14 week old control-diet fed females compared to 8 week old females, respectively). This finding indicates that the adenine diet-induced elevation of plasma phosphate at 6 weeks was in fact more pronounced than that assessed when comparing to the baseline (0 week).

Consistent with the previous literature, male mice fed the adenine-rich diet developed renal failure more severely than female mice and, therefore, had to be excluded from the study due to excessive weight loss before the end of the six-week study period. Morphological and histological analyses of data from female mice, as well as BUN levels, indicated a more progressive kidney disease in XLKO compared to WT littermates. It appears likely that adenine, rather than an intrinsic kidney pathology, is responsible for the enhanced renal injury in XLKO mice, considering that these mice did not display a similarly increased susceptibility to renal injury upon folic acid injection.

When adenine-phosphoribosyltransferase, which converts adenine to adenosine-monophosphate and inorganic pyrophosphate, is defective or when adenine concentration exceeds enzymatic capacity, adenine becomes increasingly metabolized by xanthine dehydrogenase, which converts adenine into the highly insoluble derivate 2,8-dihydroxyadenine. This molecule precipitates in the renal parenchyma, causing a crystalline nephropathy (36). XLKO phenotype is characterized by poor adaptation to feeding, early postnatal lethality, and defective glucose and energy metabolism. Furthermore, XLKO mice are lean, hypermetabolic, and show increased sympathetic nervous system activity (38,49). This hypermetabolic state might cause an increase in turnover of adenine by xanthine dehydrogenase, producing higher concentrations of its insoluble derivates and, in turn, leading to a faster progression of kidney disease. Xanthine-dehydrogenase is expressed in liver and pancreas. As XLαs is expressed in

16

WT pancreatic tissue (50), and depletion of XLαs leads to a pancreatic endocrine dysfunction (38), XLαs deficiency in pancreas might be another reason for the dissimilar progression of CKD in WT and XLKO mice. In addition, the ability to accumulate adenosine and hypoxanthine in adipose tissue (51) might act as an additional buffering mechanism for the WT animals, which have larger adipose tissue than their XLKO littermates.

Contrary to previous observations of significantly reduced plasma FGF23 levels in young XLKO pups, we detected only a slight reduction in total FGF23 plasma levels in eight-week old XLKO mice. It may be that the actions of XLαs in FGF23 synthesis are compensated by other signaling proteins in adults. It is also possible that the systemic alterations in adult XLKO mice may mask or counteract the FGF23-related phenotype resulting from the skeletal XLαs deficiency.

We did not find a significant correlation at baseline between plasma total FGF23 and phosphate levels in WT or XLKO mice. Note that a correlation between plasma FGF23 and phosphate levels at baseline has not been consistently observed, and the data remain conflicting (52-54). The positive correlation between plasma FGF23 and phosphate levels in adenine-fed XLKO mice, as opposed to WT mice, may reflect the more severe renal injury and higher FGF23 levels in XLKO mice. However, on semi-log transformation of the entire data set, we could detect a significant positive correlation in both genotypes, and the relationship between plasma total FGF23 and phosphate did not appear to differ between XLKO and WT. We could not obtain a higher degree of renal injury, which could have perhaps revealed the effect of XLαs deficiency, if any, on the plasma FGF23 response to kidney injury. Nonetheless, XLKO mice proved valuable in our experiments to assess the relative contributions of bone and bone marrow

to FGF23 levels by providing a more advanced adenine-induced renal injury model than WT mice and a wide range of plasma FGF23 values with severely elevated levels.

In folic acid injection experiments, we were able to study both males and females and observed a comparable degree of renal failure in XLKO and WT mice. Although the relationship between plasma phosphate and total FGF23 levels were not different between the two genotypes of mice, there was a modest blunting of the FGF23 elevation in XLKO males, but not females, 24 hours after folic acid injection. This finding may reflect the mild blunting of the plasma phosphate elevation in those mice at the same time point. We currently have no explanation for the mildly blunted increase in plasma phosphate and FGF23 levels in folic acid-injected XLKO males. However, although BUN levels were comparable in XLKO and WT males, the renal inflammation markers in XLKO males did not appear to be as robustly increased as in WT males, suggesting a lower degree of renal injury in XLKO than in WT males.

Upon hypoxia-stimulated EPO production, bone marrow has been found to be another important producer of FGF23 in AKI (14,15,44). In our adenine-induced CKD model, FGF23 mRNA levels increased in both bone and bone marrow, confirming that FGF23 production is stimulated in the latter, as well as in bone. However, we found FGF23 expression to be especially high in bone compared to bone marrow, both at baseline and six weeks after the adenine-rich diet. Although our quantitative RT-PCR analysis was not designed to measure absolute RNA amount, the dramatically higher FGF23 levels in bone than in bone marrow was detected by using two different house-keeping genes as reference control. Moreover, the positive linear correlation in WT mice between plasma FGF23 and bone marrow FGF23 mRNA levels was not detected in XLKO mice, which showed markedly high levels of plasma FGF23 levels upon the adenine-rich diet. The correlation was detected only after semi-log

18

transformation of data. These results may suggest that the exceedingly high levels of plasma

FGF23 reflect production in bone rather than in bone marrow. Nevertheless, our conclusion is

based on FGF23 mRNA measurements, and we realize that the vast difference between the

levels of bone and bone marrow FGF23 mRNA may not necessarily reflect the differences in

protein levels. While this possibility is important to consider, the FGF23 mRNA expression

changes observed in previous studies were concordant with protein level alterations (14,15,44).

Moreover, in agreement with our findings, a recent study showed that the serum and bone

FGF23 elevation in a similar adenine-induced renal injury model is reduced by ~90% in mice

with conditional ablation of FGF23 in mature osteoblast/osteocytes (55).

Inflammation is an important regulator of FGF23 production, and IL6 has been shown as an

important stimulator of FGF23 production in response to adenine-induced nephropathy

(11,21,22). We found unaltered IL1β mRNA levels and modestly diminished IL6 mRNA levels

in bone and bone marrow samples from WT mice following 6 weeks of adenine-rich diet. Given

that the levels of FGF23 mRNA in these tissues significantly rose during this time, our findings

suggest that local inflammation has a minor role in FGF23 production in this model of CKD. In

XLKO bone and bone marrow samples, however, the alterations observed in the levels of these

inflammatory markers were different, with mildly increased levels of IL1β mRNA and unaltered

levels of IL6 mRNA. This tendency of increased local inflammation in XLKO bone following

the adenine diet may reflect the greater degree of renal injury in those mice than in WT mice.

Our findings cannot rule out the possibility that full-blown inflammation in bone and/or bone

marrow, which could develop as a result of highly advanced renal injury, contributes to the

exceedingly high FGF23 production.

19

Recently it has been shown that the renal tubular epithelial cells also express FGF23 mRNA and protein in response to injury (12,13). Corroborating those previous observations, our data also indicate that the ectopic renal FGF23 expression is detectable concurrently with the excess FGF23 levels in plasma, i.e. soon after the impairment of renal function by the adenine-rich diet. However, the FGF23 mRNA found in kidney did not correlate with plasma FGF23 levels. This finding suggests that mechanisms governing the induction of FGF23 expression in kidney differ from those underlying the overproduction of this hormone in osseous tissues. Interestingly, renal expression of Egr1, which translates the action of FGF23 (47), correlated with plasma FGF23 levels, but not with renal FGF23 mRNA levels, strongly suggesting that the renal Egr1-response reflects global FGF23 elevation.

Despite evidence of renal injury with elevated BUN and phosphate levels, the folic acid injection did not lead to an induction of FGF23 expression in kidney. It is also possible that a longer duration of injury is required for the induction of renal FGF23 expression or that the latter requires a specific type of kidney injury, such as the one generated by adenine. Our finding, however, contrasts the data in a recent report, in which folic acid injection was stated, but not shown, to induce ectopic renal FGF23 expression (17). The latter study used the same dose and administration route of folic acid but employed a different genetic background (C57Bl/6J), which could perhaps explain the discrepancy. With respect to renal Egr1 mRNA levels in our AKI model, we did not detect an elevation in folic acid-injected XLKO males compared to vehicle-injected XLKO males. This may reflect the blunted increase of plasma FGF23 levels in those mice.

In summary, we examined the role of XLαs in adult mice regarding kidney injury-induced FGF23 production. Our investigations revealed that XLαs has a protective role in adenine-

Downloaded from https://academic.oup.com/endo/advance-article-abstract/doi/10.1210/endocr/bqz025/5638044 by University of Liverpool user on 27 November 2019

induced nephropathy, and that bone, rather than bone marrow, is a major source of excess FGF23 resulting from adenine-induced renal injury. Unlike the findings in early postnatal mice, our study did not reveal any evidence that XLαs ablation significantly impairs FGF23 production in adult mice.

References

1. Shimada T, Kakitani M, Yamazaki Y, Hasegawa H, Takeuchi Y, Fujita T, Fukumoto S, Tomizuka K, Yamashita T. Targeted ablation of Fgf23 demonstrates an essential physiological role of FGF23 in phosphate and vitamin D metabolism. *The Journal of clinical investigation*. 2004;113(4):561-568.
2. Consortium. A. Autosomal dominant hypophosphataemic rickets is associated with mutations in FGF23. *Nature genetics*. 2000;26(3):345-348.
3. Shimada T, Mizutani S, Muto T, Yoneya T, Hino R, Takeda S, Takeuchi Y, Fujita T, Fukumoto S, Yamashita T. Cloning and characterization of FGF23 as a causative factor of tumor-induced osteomalacia. *Proceedings of the National Academy of Sciences of the United States of America*. 2001;98(11):6500-6505.
4. Gattineni J, Bates C, Twombley K, Dwarakanath V, Robinson ML, Goetz R, Mohammadi M, Baum M. FGF23 decreases renal NaPi-2a and NaPi-2c expression and induces hypophosphatemia in vivo predominantly via FGF receptor 1. *American journal of physiology Renal physiology*. 2009;297(2):F282-F291.
5. Carpenter TO, Shaw NJ, Portale AA, Ward LM, Abrams SA, Pettifor JM. Rickets. *Nature reviews Disease primers*. 2017;3:17101.
6. Ramnitz MS, Gafni RI, Collins MT. Hyperphosphatemic Familial Tumoral Calcinosis. In: Adam MP, Ardinger HH, Pagon RA, Wallace SE, Bean LJH, Stephens K, Amemiya A, eds. GeneReviews((R)). Seattle (WA): University of Washington, Seattle
University of Washington, Seattle. GeneReviews is a registered trademark of the University of Washington, Seattle. All rights reserved.; 1993.
7. Larsson T, Nisbeth U, Ljunggren O, Juppner H, Jonsson KB. Circulating concentration of FGF-23 increases as renal function declines in patients with chronic kidney disease, but does not change in response to variation in phosphate intake in healthy volunteers. *Kidney Int*. 2003;64(6):2272-2279.
8. Faul C, Amaral AP, Oskouei B, Hu MC, Sloan A, Isakova T, Gutierrez OM, Aguillon-Prada R, Lincoln J, Hare JM, Mundel P, Morales A, Scialla J, Fischer M, Soliman EZ, Chen J, Go AS, Rosas SE, Nessel L, Townsend RR, Feldman HI, St John Sutton M, Ojo A, Gadegbeku C, Di Marco GS, Reuter S, Kentrup D, Tiemann K, Brand M, Hill JA, Moe OW, Kuro OM, Kusek JW, Keane MG, Wolf M. FGF23 induces left ventricular hypertrophy. *J Clin Invest*. 2011;121(11):4393-4408.
9. Scialla JJ, Xie H, Rahman M, Anderson AH, Isakova T, Ojo A, Zhang X, Nessel L, Hamano T, Grunwald JE, Raj DS, Yang W, He J, Lash JP, Go AS, Kusek JW, Feldman H, Wolf M, Chronic Renal Insufficiency Cohort Study I. Fibroblast growth factor-23 and cardiovascular events in CKD. *Journal of the American Society of Nephrology : JASN*. 2014;25(2):349-360.
10. Clinkenbeard EL, Cass TA, Ni P, Hum JM, Bellido T, Allen MR, White KE. Conditional Deletion of Murine Fgf23: Interruption of the Normal Skeletal Responses to Phosphate Challenge and Rescue of Genetic Hypophosphatemia. *Journal of bone and mineral research : the official journal of the American Society for Bone and Mineral Research*. 2016;31(6):1247-1257.

11. Bansal S, Friedrichs WE, Velagapudi C, Feliers D, Khazim K, Horn D, Cornell JE, Werner SL, Fanti P. Spleen contributes significantly to increased circulating levels of fibroblast growth factor 23 in response to lipopolysaccharide-induced inflammation. *Nephrol Dial Transplant*. 2017;32(6):960-968.

12. Mace ML, Gravesen E, Nordholm A, Hofman-Bang J, Secher T, Olgaard K, Lewin E. Kidney fibroblast growth factor 23 does not contribute to elevation of its circulating levels in uremia. *Kidney Int*. 2017;92(1):165-178.

13. Sugiura H, Matsushita A, Futaya M, Teraoka A, Akiyama K-i, Usui N, Nagano N, Nitta K, Tsuchiya K. Fibroblast growth factor 23 is upregulated in the kidney in a chronic kidney disease rat model. *PloS one*. 2018;13(3):e0191706.

14. Toro L, Barrientos V, Leon P, Rojas M, Gonzalez M, Gonzalez-Ibanez A, Illanes S, Sugikawa K, Abarzua N, Bascunan C, Arcos K, Fuentealba C, Tong AM, Elorza AA, Pinto ME, Alzamora R, Romero C, Michea L. Erythropoietin induces bone marrow and plasma fibroblast growth factor 23 during acute kidney injury. *Kidney Int*. 2018;93(5):1131-1141.

15. Rabadi S, Udo I, Leaf DE, Waikar SS, Christov M. Acute blood loss stimulates fibroblast growth factor 23 production. *American journal of physiology Renal physiology*. 2018;314(1):F132-f139.

16. Clinkenbeard EL, Hanudel MR, Stayrook KR, Appaiah HN, Farrow EG, Cass TA, Summers LJ, Ip CS, Hum JM, Thomas JC, Ivan M, Richine BM, Chan RJ, Clemens TL, Schipani E, Sabbagh Y, Xu L, Srour EF, Alvarez MB, Kacena MA, Salusky IB, Ganz T, Nemeth E, White KE. Erythropoietin stimulates murine and human fibroblast growth factor-23, revealing novel roles for bone and bone marrow. *Haematologica*. 2017;102(11):e427-e430.

17. Egli-Spichtig D, Zhang MYH, Perwad F. Fibroblast Growth Factor 23 Expression Is Increased in Multiple Organs in Mice With Folic Acid-Induced Acute Kidney Injury. *Frontiers in physiology*. 2018;9:1494.

18. Masuyama R, Stockmans I, Torrekens S, Van Looveren R, Maes C, Carmeliet P, Bouillon R, Carmeliet G. Vitamin D receptor in chondrocytes promotes osteoclastogenesis and regulates FGF23 production in osteoblasts. *The Journal of clinical investigation*. 2006;116(12):3150-3159.

19. David V, Dai B, Martin A, Huang J, Han X, Quarles LD. Calcium Regulates FGF-23 Expression in Bone. *Endocrinology*. 2013;154(12):4469-4482.

20. Tsuji K, Maeda T, Kawane T, Matsunuma A, Horiuchi N. Leptin stimulates fibroblast growth factor 23 expression in bone and suppresses renal 1alpha,25-dihydroxyvitamin D3 synthesis in leptin-deficient mice. *Journal of bone and mineral research : the official journal of the American Society for Bone and Mineral Research*. 2010;25(8):1711-1723.

21. Durlacher-Betzer K, Hassan A, Levi R, Axelrod J, Silver J, Naveh-Many T. Interleukin-6 contributes to the increase in fibroblast growth factor 23 expression in acute and chronic kidney disease. *Kidney Int*. 2018.

22. Francis C, David V. Inflammation regulates FGF23 production. *Current opinion in nephrology and hypertension*. 2016;25(4):325-332.

23. Lavi-Moshayoff V, Wasserman G, Meir T, Silver J, Naveh-Many T. PTH increases FGF23 gene expression and mediates the high-FGF23 levels of experimental kidney failure: a

23

bone parathyroid feedback loop. *American journal of physiology Renal physiology*. 2010;299(4):F882-889.

24. Rhee Y, Bivi N, Farrow E, Lezcano V, Plotkin LI, White KE, Bellido T. Parathyroid hormone receptor signaling in osteocytes increases the expression of fibroblast growth factor-23 in vitro and in vivo. *Bone*. 2011;49(4):636-643.

25. Fan Y, Bi R, Densmore MJ, Sato T, Kobayashi T, Yuan Q, Zhou X, Erben RG, Lanske B. Parathyroid hormone 1 receptor is essential to induce FGF23 production and maintain systemic mineral ion homeostasis. *FASEB journal : official publication of the Federation of American Societies for Experimental Biology*. 2016;30(1):428-440.

26. Hayward BE, Kamiya M, Strain L, Moran V, Campbell R, Hayashizaki Y, Bonthron DT. The human GNAS1 gene is imprinted and encodes distinct paternally and biallelically expressed G proteins. *Proceedings of the National Academy of Sciences*. 1998;95(17):10038-10043.

27. Kehlenbach RH, Matthey J, Huttner WB. XL alpha s is a new type of G protein. *Nature*. 1994;372(6508):804-809.

28. Bastepe M, Gunes Y, Perez-Villamil B, Hunzelman J, Weinstein LS, Juppner H. Receptor-mediated adenylyl cyclase activation through XLalpha(s), the extra-large variant of the stimulatory G protein alpha-subunit. *Molecular endocrinology (Baltimore, Md)*. 2002;16(8):1912-1919.

29. Linglart A, Mahon MJ, Kerachian MA, Berlach DM, Hendy GN, Juppner H, Bastepe M. Coding GNAS mutations leading to hormone resistance impair in vitro agonist- and cholera toxin-induced adenosine cyclic 3',5'-monophosphate formation mediated by human XLalphas. *Endocrinology*. 2006;147(5):2253-2262.

30. Mariot V, Wu JY, Aydin C, Mantovani G, Mahon MJ, Linglart A, Bastepe M. Potent constitutive cyclic AMP-generating activity of XLalphas implicates this imprinted GNAS product in the pathogenesis of McCune-Albright syndrome and fibrous dysplasia of bone. *Bone*. 2011;48(2):312-320.

31. Pignolo RJ, Xu M, Russell E, Richardson A, Kaplan J, Billings PC, Kaplan FS, Shore EM. Heterozygous inactivation of Gnas in adipose-derived mesenchymal progenitor cells enhances osteoblast differentiation and promotes heterotopic ossification. *Journal of bone and mineral research : the official journal of the American Society for Bone and Mineral Research*. 2011;26(11):2647-2655.

32. He Q, Zhu Y, Corbin BA, Plagge A, Bastepe M. The G protein alpha subunit variant XLalphas promotes inositol 1,4,5-trisphosphate signaling and mediates the renal actions of parathyroid hormone in vivo. *Sci Signal*. 2015;8(391):ra84.

33. Fernandez-Rebollo E, Maeda A, Reyes M, Turan S, Frohlich LF, Plagge A, Kelsey G, Juppner H, Bastepe M. Loss of XLalphas (extra-large alphas) imprinting results in early postnatal hypoglycemia and lethality in a mouse model of pseudohypoparathyroidism Ib. *Proceedings of the National Academy of Sciences of the United States of America*. 2012;109(17):6638-6643.

34. He Q, Shumate LT, Matthias J, Aydin C, Wein MN, Spatz JM, Goetz R, Mohammadi M, Plagge A, Divieti Pajevic P, Bastepe M. A G protein–coupled, IP3/protein kinase C pathway controlling the synthesis of phosphaturic hormone FGF23. *JCI insight*. 2019;4(17).

24

35. Tani T, Orimo H, Shimizu A, Tsuruoka S. Development of a novel chronic kidney disease mouse model to evaluate the progression of hyperphosphatemia and associated mineral bone disease. *Scientific reports*. 2017;7(1):2233.

36. Simmonds H. APRT deficiency and 2,8-DHA urolithiasis. In: CR S, ed. Metabolic and Molecular Bases of Inherited Disease. Vol 7th ed. New York, McGraw-Hill1995:1707-1724.

37. Long DA, Woolf AS, Suda T, Yuan HT. Increased renal angiopoietin-1 expression in folic acid-induced nephrotoxicity in mice. *Journal of the American Society of Nephrology : JASN*. 2001;12(12):2721-2731.

38. Plagge A, Gordon E, Dean W, Boiani R, Cinti S, Peters J, Kelsey G. The imprinted signaling protein XL alpha s is required for postnatal adaptation to feeding. *Nature genetics*. 2004;36(8):818-826.

39. Diwan V, Small D, Kauter K, Gobe GC, Brown L. Gender differences in adenine-induced chronic kidney disease and cardiovascular complications in rats. *American journal of physiology Renal physiology*. 2014;307(11):F1169-1178.

40. Xu R, Zhang L-X, Zhang P-H, Wang F, Zuo L, Wang H-Y. Gender differences in age-related decline in glomerular filtration rates in healthy people and chronic kidney disease patients. *BMC nephrology*. 2010;11(1):20.

41. Christov M, Waikar SS, Pereira RC, Havasi A, Leaf DE, Goltzman D, Pajevic PD, Wolf M, Juppner H. Plasma FGF23 levels increase rapidly after acute kidney injury. *Kidney Int*. 2013;84(4):776-785.

42. Jia T, Olauson H, Lindberg K, Amin R, Edvardsson K, Lindholm B, Andersson G, Wernerson A, Sabbagh Y, Schiavi S, Larsson TE. A novel model of adenine-induced tubulointerstitial nephropathy in mice. *BMC nephrology*. 2013;14:116.

43. Riminucci M, Collins MT, Fedarko NS, Cherman N, Corsi A, White KE, Waguespack S, Gupta A, Hannon T, Econs MJ, Bianco P, Gehron Robey P. FGF-23 in fibrous dysplasia of bone and its relationship to renal phosphate wasting. *Journal of Clinical Investigation*. 2003;112(5):683-692.

44. Daryadel A, Bettoni C, Haider T, Imenez Silva PH, Schnitzbauer U, Pastor-Arroyo EM, Wenger RH, Gassmann M, Wagner CA. Erythropoietin stimulates fibroblast growth factor 23 (FGF23) in mice and men. *Pflugers Arch*. 2018.

45. Ito N, Wijenayaka AR, Prideaux M, Kogawa M, Ormsby RT, Evdokiou A, Bonewald LF, Findlay DM, Atkins GJ. Regulation of FGF23 expression in IDG-SW3 osteocytes and human bone by pro-inflammatory stimuli. *Molecular and cellular endocrinology*. 2015;399:208-218.

46. David V, Martin A, Isakova T, Spaulding C, Qi L, Ramirez V, Zumbrennen-Bullough KB, Sun CC, Lin HY, Babitt JL, Wolf M. Inflammation and functional iron deficiency regulate fibroblast growth factor 23 production. *Kidney Int*. 2016;89(1):135-146.

47. Portale AA, Zhang MY, David V, Martin A, Jiao Y, Gu W, Perwad F. Characterization of FGF23-Dependent Egr-1 Cistrome in the Mouse Renal Proximal Tubule. *PloS one*. 2015;10(11):e0142924.

48. Zierk J, Arzideh F, Rechenauer T, Haeckel R, Rascher W, Metzler M, Rauh M. Age- and Sex-Specific Dynamics in 22 Hematologic and Biochemical Analytes from Birth to Adolescence. *Clinical Chemistry*. 2015;61(7):964-973.

25

49. Xie T, Plagge A, Gavrilova O, Pack S, Jou W, Lai EW, Frontera M, Kelsey G, Weinstein LS. The alternative stimulatory G protein alpha-subunit XLalphas is a critical regulator of energy and glucose metabolism and sympathetic nerve activity in adult mice. *The Journal of biological chemistry*. 2006;281(28):18989-18999.

50. Pasolli HA, Klemke M, Kehlenbach RH, Wang Y, Huttner WB. Characterization of the extra-large G protein alpha-subunit XLalphas. I. Tissue distribution and subcellular localization. *The Journal of biological chemistry*. 2000;275(43):33622-33632.

51. Kather H. Purine accumulation in human fat cell suspensions. Evidence that human adipocytes release inosine and hypoxanthine rather than adenosine. *The Journal of biological chemistry*. 1988;263(18):8803-8809.

52. Burnett SM, Gunawardene SC, Bringhurst FR, Juppner H, Lee H, Finkelstein JS. Regulation of C-terminal and intact FGF-23 by dietary phosphate in men and women. *Journal of bone and mineral research : the official journal of the American Society for Bone and Mineral Research*. 2006;21(8):1187-1196.

53. Marsell R, Mirza MA, Mallmin H, Karlsson M, Mellstrom D, Orwoll E, Ohlsson C, Jonsson KB, Ljunggren O, Larsson TE. Relation between fibroblast growth factor-23, body weight and bone mineral density in elderly men. *Osteoporosis international : a journal established as result of cooperation between the European Foundation for Osteoporosis and the National Osteoporosis Foundation of the USA*. 2009;20(7):1167-1173.

54. Mitchell DM, Juppner H, Burnett-Bowie SM. FGF23 Is Not Associated With Age-Related Changes in Phosphate, but Enhances Renal Calcium Reabsorption in Girls. *The Journal of clinical endocrinology and metabolism*. 2017;102(4):1151-1160.

55. Clinkenbeard EL, Noonan ML, Thomas JC, Ni P, Hum JM, Aref M, Swallow EA, Moe SM, Allen MR, White KE. Increased FGF23 protects against detrimental cardio-renal consequences during elevated blood phosphate in CKD. *JCI insight*. 2019;4(4).

26

Figure Legends:

Figure 1. XLαs and FGF23 levels in WT and XLKO mice, as well as their weights and survival during adenine-rich diet.

Eight-week old WT and XLKO mice were euthanized and XLαs-mRNA levels were measured in bone (A) and bone marrow tissue (B).

Plasma samples from 8 week-old WT and XLKO females were collected and levels of total (C) and intact (D) FGF23 were determined. Unpaired Student's t-test (two-tailed) was used for statistical comparison. Welch's Test was used for unequal variances.

(E) Females and males were weighed on a weekly basis and the weight progression was compared between the genotypes and the diets. Figure (F) shows the survival data of males and females of both genotypes during the adenine-rich diet.

(A) WT n=3, XLKO n=3; (B) WT n=3, XLKO n=3

(C) WT n=18, XLKO n=23; (D) WT n=9, XLKO n=11

(E) female WT adenine n=12, control n=10; females XLKO adenine n=13, control n=12; male WT adenine n=4, control n=6; male XLKO adenine n=8, control n=7;

(F) females n=25, males n=12

Figure 2. The effect of the adenine-rich diet on kidneys.

(A) Kidneys from three female WT and three female XLKO mice we harvested at 0, 1, or 2 weeks of adenine diet. Pale spots on the kidney surface display an early onset of the kidney damage. Morphological comparison reveals a faster progressing kidney injury in XLKO mice starting at 1 week of Adenine Diet. At 6 weeks (B), kidneys of adenine-fed mice were shrunk and pale with an irregular surface. (C) Histological analysis revealed an extensive tubular

27

dilation upon six weeks of adenine diet with more pronounced kidney damage in the XLKO

mice compared to WT mice. (For B, C) Six WT mice receiving control diet, six WT mice

receiving adenine diet, seven XLKO mice receiving control diet and nine XLKO mice receiving

adenine diet were compared for histological and morphological analysis. Representative

histology sections are shown. (D, E) Plasma phosphate and BUN levels in WT and XLKO mice

following adenine-rich diet. Plasma samples were collected from WT and XLKO mice before

and after 6 weeks of adenine or control diet. BUN (D) and Phosphate (E) levels were obtained.

Unpaired Student's t-test (two-tailed) was used, with or without Welch's Test (for unequal

variances), followed by Bonferroni correction of the p values for multiple comparisons. (D) 0

week WT n=11, XLKO=11; 6 week WT n=11, XLKO=11; (E) 0 week WT n=14, XLKO=12; 6

week WT n=11, XLKO=11;

Figure 3. Time-course of plasma FGF23 elevation, and the relationship between FGF23, plasma phosphate and BUN.

8 week-old WT and XLKO mice were fed with 0.2% adenine-rich or control diet for 6 weeks.

Plasma samples were collected at different timepoints. (A) The time course of total FGF23 is

shown in WT (blue) and XLKO (red) plasma samples at 0, 1, 2, 4 and 6 weeks of adenine (A)

and control diet (B). Two-way ANOVA multiple comparison analysis was used for statistical

analysis. (C) iFGF23 levels are shown after 6 weeks of control or adenine diet. Unpaired

Student's t-test (two-tailed) was used for statistical comparison between the genotypes. Linear

regression analysis was performed between total plasma FGF23 and phosphate in WT and

XLKO mice before (0 wk, D) and after six weeks of adenine diet (E). Both timepoints were

combined and linear regression analysis was performed between the genotypes before (F) and

28

after semi-log transformation of total plasma FGF23 (G). The Pearson correlation coefficient was calculated. (A) WT adenine n=8, XLKO adenine n=10; (B) WT control n=9, XLKO control n=12; (C) Control WT n=10, XLKO=12; Adenine WT n=9, XLKO=11; (D) WT n=9, XLKO n=10; (E) WT n=9, XLKO n=10; (F, G) WT n=18, XLKO n=20.

Figure 4. Bone and bone marrow FGF23 mRNA levels in response to adenine-rich diet.
8 week-old WT and XLKO mice were fed with 0.2% adenine or control diet for 6 weeks. Cortical bone (A, C) and bone marrow (B, D) tissue samples were collected and FGF23 mRNA levels were determined at 6 weeks by using beta-actin (A, B) or GAPDH (C, D) as reference control. Unpaired Student's t-test (two-tailed) was used for statistical analysis. Welch's Test was used for unequal variances. (E) Ratio of bone-to-bone marrow FGF23 mRNA level after 6-weeks of adenine diet, measured relative to either β-actin or GAPDH in individual mice from both WT and XLKO groups. (A) Control WT n=5, XLKO=5; Adenine WT n=4, XLKO=7; (B) Control WT n=4, XLKO=6; Adenine WT n=5, XLKO=9; (C) Control WT n=5, XLKO=5; Adenine WT n=4, XLKO=7; (D) Control WT n=5, XLKO=5; Adenine WT n=5, XLKO=7; (E) n=7 for both groups.

Figure 5. The relationship between plasma FGF23 and bone or bone marrow FGF23 mRNA levels in WT and XLKO mice.
Linear regression analysis was performed between plasma FGF23 and tissue FGF23 mRNA expression in bone (A-C) and bone marrow (D-F), determining the Pearson correlation coefficient. Bone marrow FGF23 was compared to log (plasma FGF23) in XLKO (G) and both genotypes (H) performing linear regression analysis and determining the Pearson correlation

29

coefficient. (A) WT n=9 (Control n=5, Adenine n=4), (B) XLKO n=11 (Control n=5, Adenine n=6); (C) WT + XLKO n=20, (D) WT n=9 (Control n=4, Adenine n=5), (E) XLKO n=14 (Control n=6, Adenine n=8), (F) WT + XLKO n=23, (G) XLKO n=14 (Control n=6, Adenine n=8), (H) WT + XLKO n=23.

Figure 6. Markers of inflammation in bone, bone marrow and kidney tissue following 6 weeks of adenine-rich diet.

Eight-week old WT and XLKO mice were fed with 0.2% adenine (gray bars) or control (black bars) diet for 6 weeks. Cortical bone (A), bone marrow (B) and kidney samples (C) were collected and IL1β and IL6 mRNA levels were determined using β-actin as reference control. Unpaired Student's t-test (two-tailed) was used for statistical comparisons. Welch's Test was used for unequal variances.

(A) Control WT n=5, XLKO=5; Adenine WT n=5, XLKO=7; (B) Control WT n=5, XLKO=6; Adenine WT n=6, XLKO=9; (C) Control WT n=10, XLKO=12; Adenine WT n=9, XLKO=11.

Figure 7. Adenine-induced alterations in kidney, including the induction of FGF23 mRNA expression.

Eight-week old WT and XLKO mice were fed with 0.2% adenine (gray bars) or control (black bars) diet and kidney samples were collected after 1, 2 or 6 weeks. FGF23 (A, B) and Egr (C, D) mRNA expression levels were determined using β-actin as reference control. ND = none detected. Linear relationship between kidney Egr1 mRNA and total plasma FGF23 levels (E) or kidney FGF23 mRNA expression (F) was examined by correlation analysis using the Pearson correlation coefficient. Unpaired Student's t-test (two-tailed) was used for statistical

30

comparisons. Welch's Test was used for unequal variances. (A) WT: 1 week Adenine n=3; 2 week Adenine n=3; 6 week Adenine n=10; (B) XLKO: 1 week Adenine n=3; 2 week Adenine n=3; 6 week Adenine n=10; (C) WT: 1 week Adenine/Control n=3; 2 week Adenine/Control n=3; 6 week Adenine/Control n=9; (D) XLKO: 1 week Adenine/Control n=3; 2 week Adenine/Control n=3; 6 week Adenine n=9; 6 week Control n=11; (E) n=17 (WT n=8, XLKO n=9); (F) n=17 (WT n=8, XLKO n=9).

Figure 8. Plasma phosphate, BUN, and plasma FGF23 dynamics after folic acid-induced acute kidney injury.

12-week old WT and XLKO males and females were injected subcutaneously with folic acid and euthanized after 24 hours. Blood samples were collected 0, 2, 8 and 24 hours after folic acid injection and levels of plasma phosphate (A, D), BUN (B, E) and FGF23 (C, F) were determined. Two-way ANOVA multiple comparison analysis was used for statistical analysis. (A) WT n=10, XLKO n=10; (B) WT n=10, XLKO n=10; (C) WT n=9, XLKO n=10; (D) WT n=11, XLKO n=8; (E) WT n=11, XLKO n=8; (F) WT n=11, XLKO n=7.

Figure 9. The relationship between plasma FGF23 and phosphate levels after folic acid-induced acute kidney injury.

12-week old WT and XLKO males and females were injected subcutaneously with folic acid and euthanized after 24 hours. Blood samples were collected 0, 2, 8 and 24 hours after folic acid injection. Levels of plasma FGF23 and phosphate were obtained. Data points of all four timepoints were pooled and linear regression analysis was performed determining the Pearson

31

correlation coefficient (A, C). Panels B and D display the semilogarithmic graphs of data in panels A and C.

(A, B) WT n=36 (9 mice), XLKO n=40 (10 mice); (C, D) WT n=44 (11 mice), XLKO n=28 (7 mice).

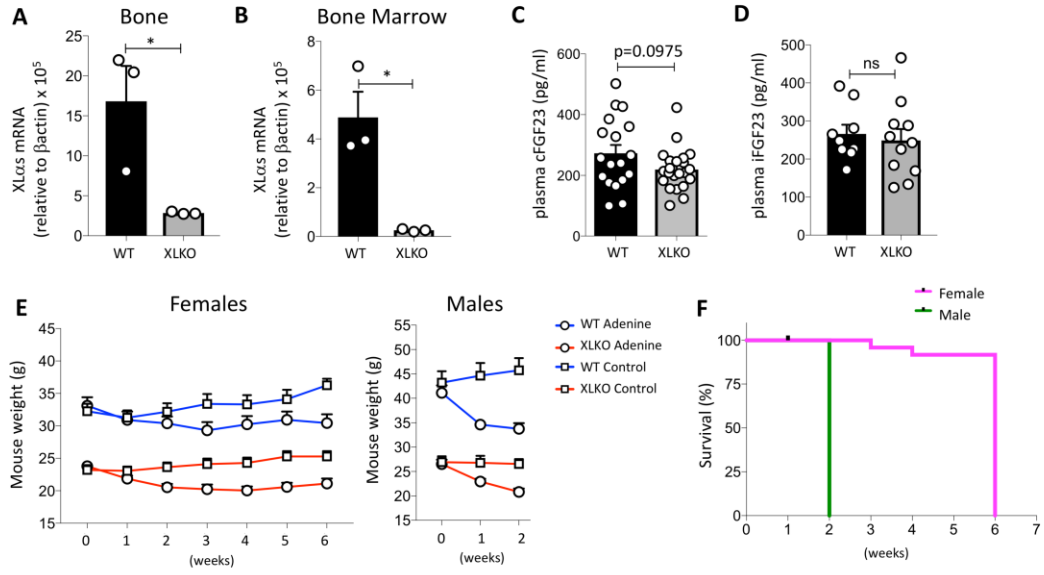**Figure 10. Folic acid-induced alterations of inflammation markers and Egr1 expression in kidney.**

12-week old WT and XLKO males and females were injected subcutaneously with vehicle (control) or folic acid (FA) and euthanized after 24 hours. Kidney samples were collected and mRNA expression levels of IL6 (A, D), IL1β (B, E) and EGR1 (C, F) were determined using β-Actin as reference control. Unpaired Student's t-test (two-tailed) was used for statistical comparisons. Welch's Test was used for unequal variances, followed by Bonferroni correction of p values.

(A) WT control n=8, FA n=9; XLKO control n=10, FA n=9; (B) WT control n=9, FA n=10; XLKO control n=10, FA n=8; (C) WT control n=8, FA n=11; XLKO control n=9, FA n=8; (D) WT control n=9, FA n=11; XLKO control n=11, FA n=9; (E) WT control n=8, FA n=10; XLKO control n=9, FA n=10; (F) WT control n=11, FA n=15; XLKO control n=12, FA n=10.

Figure 1

Figure 2

Figure 3

35

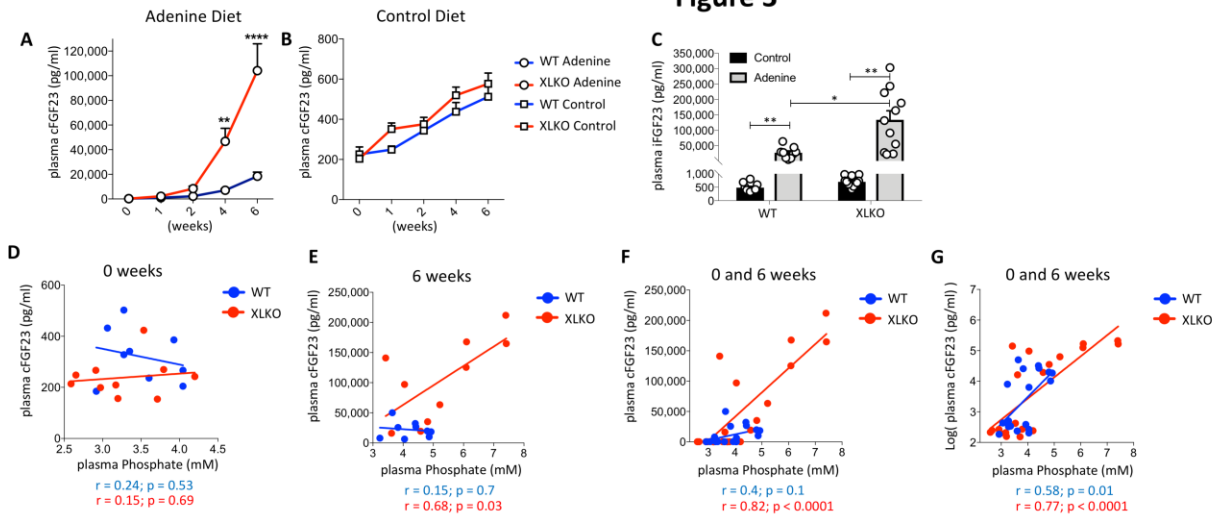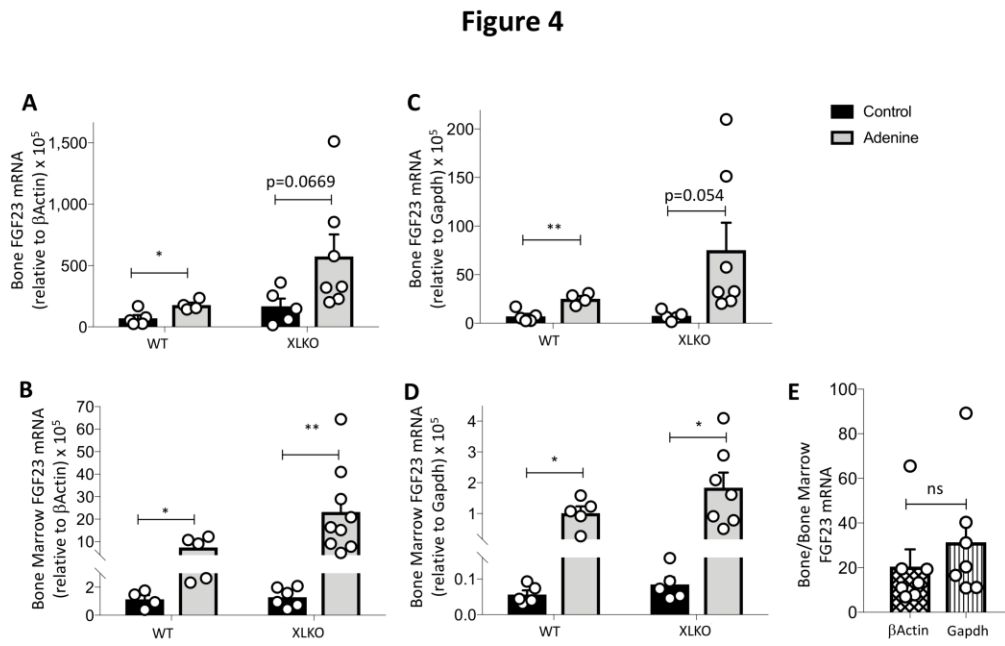**Figure 4**

Figure 5

37

Figure 6

Figure 7

Figure 8

Figure 9

A — Females
plasma cFGF23 (pg/ml) vs plasma Phosphate (mM)
r = 0.89; p < 0.001
r = 0.73; p < 0.001

B — Females
Log(plasma cFGF23 (pg/ml)) vs plasma Phosphate (mM)
WT
XLKO
r = 0.93; p < 0.001
r = 0.86; p < 0.001

C — Males
plasma cFGF23 (pg/ml) vs plasma Phosphate (mM)
r = 0.77; p < 0.001
r = 0.75; p < 0.001

D — Males
Log(plasma cFGF23 (pg/ml)) vs plasma Phosphate (mM)
slopes are significantly different p=0.04
r = 0.83; p < 0.001
r = 0.805; p < 0.001

Figure 10